International Journal of Engineering

Journal Homepage: www.ije.ir

Synthesis and Characterization of Anatase-coated Multiwall Carbon Nanotube for Improvement of Photocatalytic Activity

F. Kordhaghi, S. K. Sadrnezhaad*

Department of Materials Science and Engineering, Sharif University of Technology, Tehran, Iran

PAPER INFO

Paper history:
Received 22 May 2016
Received in revised form 09 February 2017
Accepted 09 February 2017

Keywords:
Nano-photocatalyst
Anatase
Titanium Dioxide
Carbon Nanotube
Nanocomposite

ABSTRACT

Sol-gel technique was used to coat multiwall carbon nanotubes (MWCNTs) with anatase titania to increasing the surface area and improve the photocatalytic activity of TiO_2. Room temperature ballistic conduct of MWCNT combined with semiconducting behavior of anatase brought about a photocatalytic improvement of ~37 % with respect to the highest methyl orange decolorization flair. For characterization and photocatalytic efficiency determination, X-ray diffraction (XRD), field emission (FE) scanning electron microscopy (SEM), x-ray photoelectron spectroscopy (XPS), diffuse reflectance spectroscopy (DRS) and ultraviolet visible (UV-vis) spectroscopy were rehearsed. Attachment of anatase nanoparticles onto 30 wt % functionalized CNTs resulted in 99.72% methyl orange decolorization by 160 min irradiation with 8 W ultraviolet lamp. This value was fourfold greater than pure TiO_2 nanoparticles and much greater than the values reported in the literature. This improvement was attributed to larger surface area, lower charge recombination and superior crystal structure and stimulated visible-light shifting due to presence of Ti–O–C bond.

doi: *10.5829/idosi.ije.2017.30.04a.12*

1. INTRODUCTION

Semiconducting photocatalysts have attracted much attention due to their profound cleanliness and insightful oxidation/reduction reactions under atmospheric conditions [1-10]. Remarkable industrial growth together with environmental conservation of air and water [2-5], sensor application [6-8], solar cell improvement [9, 10], hydrogen production [11], bacterial disinfection [12] and self-cleaning of the exposed surfaces [13-15] are recognizable novel aspects.

After the discovery of the anatase photoactivity, semiconductor photocatalysis has received enormous attention [1]. Anatase is notable as best semiconducting photocatalyst. Its superb efficiency, nontoxic conduct, electronic behavior, optical performance, chemical stability and low cost have attracted great attention [3, 16]. However, limitations like large band-gap, small quantum yield and substantial charge recombination have reduced its gains [16-18]. To overcome these drawbacks, thoughtful tasks have been envisioned [19-27]. Enhancement of photocatalytic activity with sensitization [19, 20], coupling with conductive particles [21-27], doping with metallic elements [28-30] and even metallization [31-34] have been proposed.

TiO_2 irradiation with UV light results in generation of photoelectrons and holes which can decompose toxic pollutants [35]. These properties are reflections of TiO_2 electronic structure. In perfect TiO_2 crystal structure, the electrons are kicked out of the valence band toward the conduction band by irradiated waves. Defect creation by modifiers addition results in new electronic level formation. This level can be adjusted in the middle of the ordinary band gaps [21]. Activation of TiO_2 by less energy waves such as visible light would thus become practically conceivable.

Multiwall carbon nanotube is a suitable material for coupling with TiO_2 photo-absorber [36]. This material has hollow layered structure, mechanical strength; large specific surfaces, considerable electrical conductivity, high adsorption capacity and great potential for

*Corresponding Author's Email: sadrnezh@sharif.edu (S. K. Sadrnezhaad)

Please cite this article as: F. Kordhaghi, S. K. Sadrnezhaad, Synthesis and Characterization of Anatase-coated Multiwall Carbon Nanotube for Improvement of Photocatalytic Activity, International Journal of Engineering (IJE), TRANSACTIONS A: Basics Vol. 30, No. 4, (April 2017) 543-550

structural reconstruction. Combination of photocatalytic activity of anatase TiO_2 with high adsorption capacity and electron transport capability of MWCNT introduce them as excellent wave absorbers for photocatalytic applications in both ranges of UV and visible light.

Previous researchers have focused on photocatalytic activity of TiO_2 having less than 5 wt% CNT. According to some researchers, presence of larger quantities of CNT with TiO_2 causes diminution of the photocatalytic efficiency of the photocatalyst [16, 37-39]. In the present work, the photocatalytic activity of CNT-(anatase) TiO_2 nanocomposite having up to 30 wt% CNT is investigated. For nanocomposite synthesis, a simple additive-less sol-gel method performed at the ambient temperature is deployed. Photocatalytic efficiency of the synthesized nanocomposite is measured by determination of the methyl orange degradation. Improving effects are observed by utilization of the non-clustering CNT rich-anatase coated product.

2. EXPERIMENTAL PROCEDURE

2. 1. Raw Materials Multiwall carbon nanotubes with average outer diameter of 20 nm, length of ~30μm, purity of >95 % and specific surface area of 152 m^2/g were provided by Neutrino Corporation of Iran. Tetraisopropyl orthotitanate (TTIP), ethanol (analytical grade), hydrochloric acid (37%), nitric acid (65%) and sulfuric acid (96%) were purchased from Merck (Germany). Dye model solution containing 5 mg/L of methyl orange was prepared by using distilled water.

2. 2. TiO_2 Nanopowder TiO_2 nanopowder was synthesized by sol-gel method. TTIP-ethanol mixture of 1:3 volume ratio was stirred for 30min. Another solution containing ethanol, distilled water and HCl with volume ratio 20:1:1 was drop-wise added into the TTIP-ethanol mixture until its volume ratio became 5:35:1:1 TTIP:ethanol:water:HCl. The mixture was stirred at room temperature for 5h. The sol was then dried by heating at 70°C for 24h and then annealed at 430°C for 2h to form TiO_2 of anatase structure.

2. 3. CNT Functionalization Mixture of CNT in nitric-sulfuric acids (1:1 volumetric ratio) was sonicated at room temperature for 30min and then refluxed at 100°C for 5h. The solution was then removed and the CNTs were washed with distilled water to totally neutralize the remained traces of acid on samples. The CNTs were dried at 35°C for 48h and FT-IR spectrometric functionalization was then determined.

2. 4. Preparation of CNT-anatase TiO_2 Nanocomposite For synthesis of the CNT-anatase nanocomposite, TTIP-ethanol mixture of 1:3 volume ratio was stirred for 30min. Functionalized CNT was added to ethanol-distilled water-HCl solution and then sonicated until the CNTs were completely dispersed. The first solution was then added and the whole thing was sonicated. Samples having 1, 5, 10, 20 and 30 weight percent CNTs were annealed under inert Ar atmosphere.

2. 5. Photocatalytic Tests A 25×30×40 cm^3 photoreactor having 8W UVC lamp was assembled for measurement of the photocatalytic activity of the samples. Decolorization rate of methyl orange aqueous solution was measured at room temperature. A model solution of 5mg/L methyl orange was continuously stirred with 0.7g/L of the prepared photocatalyst both charged into the reactor. The source of light (UVC lamp) was located 7cm away from the CNT-anatase nanocomposite. Samples were taken out periodically from the reactor for colorimetric test. Dye concentration near the samples was determined by 6705 UV-Vis spectrophotometer (JENWAY-UK).

Absorbance values of all solutions were obtained from UV-vis spectra at certain times. According to the Beer-Lambert law (A=εlc, A: absorbance, ε: absorptivity coefficient, l: path length, c: concentration), solution concentration relates directly to the absorbance. Therefore, we can use the following equation to calculate the degradation rate (η):

$$\eta\ (\%) = (1- c/c_0)\times 100 = (1- A/A_0)\times 100 \quad (1)$$

where c, c_0, A and A_0 are concentration of dye after a certain irradiation time, concentration of dye prior to irradiation, absorbance after a certain irradiation time and initial absorbance, respectively.

2. 6. Photocatalyst Characterization The crystal phase and crystallite size of the TiO_2 particles were characterized by XRD on a Panalytical-X'Pert Pro MPD (The Netherlands) equipped with Cu Kα radiation source. FE-SEM was conducted on a Tescan microscope (USA) operating at 5 kV for CNTs and 15 kV for TiO_2 nanoparticles and synthesized nanocomposites after being sputtered with gold. The functionalization of the CNT particles was studied by a Bruker-vertex FT-IR spectrometer (Germany). X-ray photoelectron spectroscopy (XPS) was employed to investigate the chemical state of the sample using a hemispherical analyzer from Specs EA10 plus with Al Kα X-ray (hν=1486.6 eV) radiation operated at vacuum better than 10^{-7} Pa. Diffuse reflectance spectroscope (DRS) using Avantes Avaspec-2048-TEC spectrometer was used to determine band gap of the samples based on the Kubelka-Munk model.

3. RESULTS AND DISCUSSION

3. 1. XRD XRD images of all samples were similar.

Figure 1 compares the spectrum of TiO_2-30 wt% CNT with pure TiO_2. Both images have ten peaks at ~25.3°, 37.9°, 48.1°, 53.9°, 55.1°, 62.6°, 68.8°, 70.3°, 75.2° and 82.8°, which correspond to diffractions from (101), (004), (200), (105), (211), (204), (116), (220), (215) and (224) tetragonal anatase crystal planes. The sharp and intense (002) reflection of CNT at about 2θ≈26° [16, 36] is not observed in the pattern. Homogeneous dispersion of CNT [37, 38] and formation of a complete TiO_2 coating on the CNTs can cause the nonexistence of CNT peaks in the XRD patterns.

Using the Scherrer equation, the size of the anatase crystallites was calculated ($d = 0.9\lambda/\beta \cos\theta$) with regard to the (004) peak of the anatase phase which has no overlap with the CNT particles. The crystallite size of pure TiO_2 and TiO_2-30 wt% CNT was evaluated 9.7 and 6.6nm, respectively. The size of anatase crystallites decreased with addition of CNT to TiO_2.

Some investigators have confirmed that the size of the anatase crystallites decreases with increasing the CNT content [16, 37, 39, 40]. This can be due to the effect of interaction between hydroxyl functional groups in the hydrolyzed TiO_2 precursor and –OH or –COOH groups (as defects) on the surface of the functionalized CNTs. The mentioned defects of the CNTs act as suitable sites for anatase crystallites to grow grains that cause the deposition of the TiO_2 crystallites on the surface of CNTs instead of CNT dispersion in TiO_2 lattice. Thus, CNT plays an important role in reducing crystallite size of the TiO_2 and preventing its agglomeration [40].

3. 2. FE-SEM Figure 2 shows the FE-SEM images of (a) pure TiO_2, (b) 5 wt% CNT-TiO_2 sample and (c) 30 wt% CNT-TiO_2 nanocomposite. Full coverage of CNTs by TiO_2 particles is due to existence of enough suitable active sites on the surface of the nano tubes. As previously mentioned (XRD results), the size of the TiO_2 nanoparticles decreased with the CNT content. This result was confirmed by FE-SEM images.

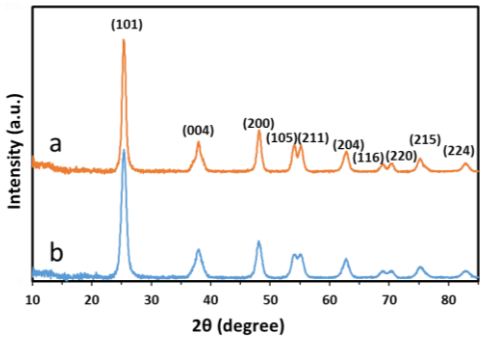

Figure 1. XRD spectra of (a) pure TiO_2, (b) TiO_2-30wt. %CNT

Figure 2(c) is a typical example which indicates reduction of TiO_2 particle size and absence of TiO_2 agglomeration at high CNT content. This result was confirmed by comparison of the crystallite size of pure TiO_2 with 30 wt% CNT-TiO_2 obtained from XRD patterns.

Average size of one hundred particles indicated 24.39 nm for pure TiO_2, 20.49 for 5 wt% CNT-TiO_2 and 6.76 nm for 30 wt% CNT-TiO_2. Furthermore, coverage of the nanotubes with TiO_2 increased the specific surface area of the samples.

The significant difference between crystallite sizes obtained from XRD patterns (9.7nm) with FE-SEM determinations (24.39nm) for pure TiO_2 indicated agglomeration of the particles. Similar comparison for 30 wt% CNT-TiO_2 nanocomposite (6.6 versus 6.76 nm) indicated preventive effect of 30 wt% CNT on TiO_2 particles agglomeration. It was therefore concluded that the most effective surface area and the greatest photocatalytic effect can be obtained in samples having 30 wt% CNT coated with TiO_2. Presence of larger amounts of nanotubes reduces the effective surface area of TiO_2 particles and hence decreases their catalytic effect.

3. 3. XPS Figure 3 shows x-ray photoelectron spectroscopy (XPS) spectra of the nanocomposite 30 wt% CNT-TiO_2 samples. General spectrum of the sample displays intensity peaks of the elements Ti, O and C present on the surface of nanocomposite (Figure 3a). Figure 3b shows high resolution XPS spectra of Ti2p ($Ti2p_{1/2}$ and $Ti2p_{3/2}$ of Ti^{4+} being at binding energies of 465.6 and 459.9 eV, respectively) which are higher than those of pure anatase ($Ti2p_{1/2}$: 464.5 eV, $Ti2p_{3/2}$: 458.8 eV [41]).

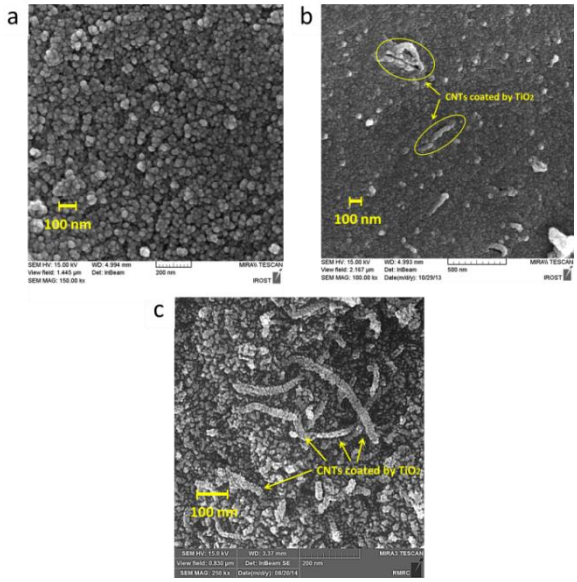

Figure 2. FE-SEM images of (a) pure TiO_2, (b) 5 wt % CNT-TiO_2 and (c) 30 wt % CNT- TiO_2 nanocomposite samples

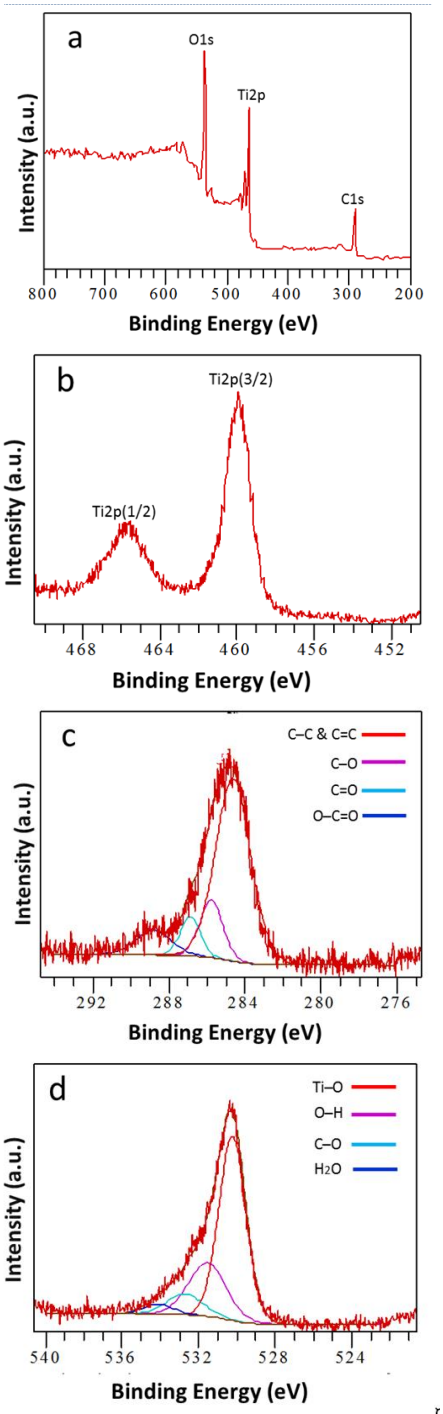

Figure 3. XPS spectra of 30 wt% CNT-TiO_2 surface: (a) general spectrum, and (b to d) high resolution spectra of Ti2p, C1s and O1s, respectively

$Ti2p_{1/2}$ and $Ti2p_{3/2}$ peaks splitting of 5.7eV is consistent with the Ti^{4+} normal state [41, 42]. The small shifting of 1.1eV seems therefore to be due to the difference in the environment conditions of pure anatase with the synthesized nanocomposite sample which contains Ti−O−C bonds. C1s high resolution XPS spectrum shown in Figure 3c is well fitted into the following four peaks: C−C (or C=C), C−O, C=O and O−C=O bonds located at binding energies of 284.6, 285.8, 286.9, 288.8 eV, respectively.

C− C and C=C bonds are attributed to CNT and graphite, respectively, and the C−O, C=O and O−C=O bonds are the chemical groups on the surface of functionalized CNTs to create bond with TiO_2. It can be seen that no peak appears at lower binding energy of 284.6eV, which means that there is no Ti−C bond on the surface of CNTs. O1s high resolution XPS spectrum of Figure 3d deconvolutes with four peaks.

The peaks at 534.1eV and 530.3eV are attributed to H_2O molecules on the surface of the sample and Ti−O bond of anatase TiO_2, respectively. Other peaks at 531.6 and 532.8eV are ascribed to O−H (hydroxyl group) and C−O bonds, respectively. From the XPS results, it can be concluded that Ti− O− C carbonaceous bonds (combination of Ti− O bond at 530.3 eV with O− C bonds at C1s and O1s spectra) are formed at the TiO_2/CNT interface and there is a close contact between anatase nanoparticles and CNTs.

3. 4. DRS Diffuse reflectance spectroscopy was performed to measure the band gaps of pure TiO_2 and 30 wt% CNT-TiO_2 nanocomposite samples. Figure 4 illustrates reflectance vs. wavelength curves. Using the Kubelka-Munk model, 394 and 429nm absorption wavelengths and 3.15, 2.90eV energy gaps (E_g) were obtained for TiO_2 and 30 wt% CNT-TiO_2 nanocomposite, respectively. It is observable that the absorption of the prepared composite is shifted to larger wavelengths in the visible range (λ > 380nm). Thus, restrictions on the use of UV light for TiO_2 photocatalysts is eliminated and photocatalytic activity in visible light becomes plausible.

A probable reason for this is the formation of the Ti−O−C bonds that introduce a medium energy state near the valence band of TiO_2 that cause to extend the absorption towards the longer wavelengths and improve the visible light photodegradation ability [43, 44].

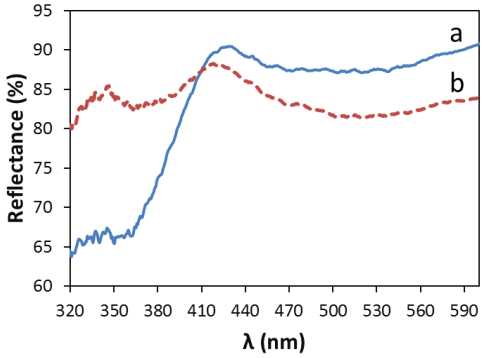

Figure 4. DRS spectra of (a) pure TiO_2 and (b) 30 wt% CNT-TiO_2 nanocomposite

3. 5. Photocatalytic Activity Photodegradation ability of the synthesized nanocomposite was determined by measuring its decoloring effect under UV light irradiation on 5mg/L methyl orange aqueous solution. Figure 5 compares the decolorization effect of pure TiO_2 and CNT-TiO_2 nanocomposites of different CNT contents with photocatalyst-less photolysis sample. Direct photolysis sample (Figure 5a) indicates a 1.34 percent decolorization after 160 min irradiation. Pure TiO_2 (Figure 5b) increases the decolorization rate significantly to 23.73% in 160 minutes. Coated CNT with anatase TiO_2 escalates the photodegradation rate, further.

With increasing CNT content of photocatalyst nanocomposite, decolorization rate greatly increases (Figures 5c to 5g). This can be due to provision of large surface area to the photocatalytic reaction, absorption of dye molecules by CNTs and ceasing of the electron-hole recombination processes. It can be seen that 30 wt% CNT-TiO_2 (Figure 5g) has the highest effect among the tested samples showing 96% and 99.72% decolorization after 80 and 160 minutes, respectively.

Based on our analysis, CNT causes enhancement of the available surface area for the photocatalytic reactions.

Furthermore, CNT has high electron conductivity and large electron storage capacity. Hence, after favorable adsorption of methyl orange on the photocatalyst surface, CNTs can transfer the photogenerated electrons from the conduction band of the anatase phase to the CNT surface due to its lower Fermi level and photogenerated holes remain in the valence band of the former. As a result, the photogenerated electrons-holes recombination is prevented and photocatalytic activity increases [45, 46].

3. 6. Photodegradation Kinetics The CNT-TiO_2 anatase phase decolorization effect on methyl orange followed the following pseudo first order kinetics:

$$r = -\frac{dC}{dt} = kc \quad (2)$$

where r, C, t and k refer to the rate, dye concentration, time and apparent rate constant of the decolorization reaction, respectively. The following equation is derived from Equation (2):

$$-\ln\left(\frac{C}{C_0}\right) = kt \quad (3)$$

Plots of - ln (C/C_0) versus t are leaner with constant slopes specifying the value of k for each photocatalyst sample. Using Equations (1) and (3), the following relation is obtained for calculation of the ideal decolorization percentage (η^*):

$$\eta^* = (1 - e^{-kt}) \times 100 \quad (4)$$

Figure 6 compares the ideal decolorization percentage of different samples.

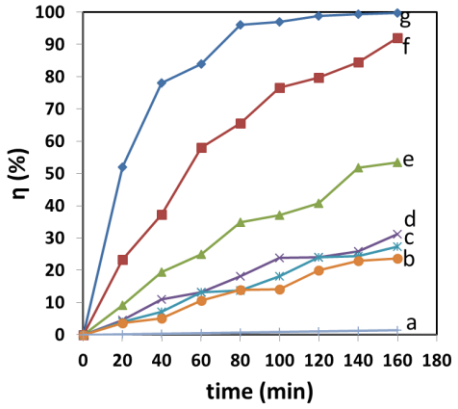

Figure 5. Comparison of photodegradation rate of methyl orange: (a) without catalyst (direct photolysis), (b) with pure TiO_2 catalyst, (c) with 1 wt% CNT-TiO_2, (d) with TiO_2-5wt. %CNT-TiO_2, (e) with 10 wt% CNT-TiO_2, (f) with 20 wt% CNT-TiO_2 and (g) with 30 wt% CNT-TiO_2

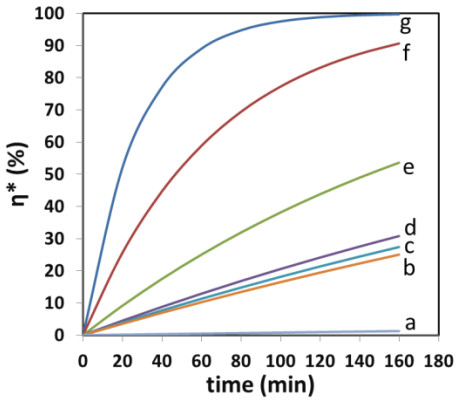

Figure 6. Ideal photodegradation percentage of methyl orange against irradiation time: (a) without catalyst (direct photolysis), (b) with pure TiO_2 catalyst, (c) with 1 wt% CNT-TiO_2, (d) with TiO_2-5wt. %CNT-TiO_2, (e) with 10 wt% CNT-TiO_2, (f) with 20 wt% CNT-TiO_2 and (g) with 30 wt% CNT-TiO_2

4. CONCLUSIONS

TiO_2 of anatase structure was synthesized by modified sol-gel method and added to CNT particles functionalized with 1:1 nitric: sulfuric acids mixtures. Nanocomposite CNT coated with TiO_2 resulted in significant photocatalytic activity improvement especially at higher CNT contents of up to 30 wt%. Carbon nanotubes decreased the crystallite size of TiO_2 and prevented agglomeration of oxide particles attached to CNTs. With large CNT contents, the band gap of the anatase-coated CNT was less than pure TiO_2 due to the formation of Ti−O−C bonds at the oxide-CNT interface. Medium energy state with red-shifting of the absorption curves was obtained. Visible light activation with high photocatalytic effect was thus resulted from utilization

of 30 wt% CNT coated with Anatase TiO_2 in methyl orange decolorization reaction. The strength of these effects appeared significantly greater than pure TiO_2 and photocatalysts with lower CNT contents. The CNTs seemed preventing charge recombination by trapping of the photogenerated electrons as well as increasing the contact areas of the samples.

5. ACKNOWLEDGEMENTS

The authors appreciate Bionano Laboratory of the Sharif University of Technology, Nanotechnology Initiative Council and Iran National Science Foundation for their assistance and support of this research.

6. REFERENCES

1. Fujishima, A., "Electrochemical photolysis of water at a semiconductor electrode", ***Nature***, Vol. 238, (1972), 37-38.
2. Bianchi, C.L., Pirola, C., Galli, F., Cerrato, G., Morandi, S. and Capucci, V., "Pigmentary TiO_2: A challenge for its use as photocatalyst in nox air purification", ***Chemical Engineering Journal***, Vol. 261, (2015), 76-82.
3. Andreozzi, R., Caprio, V., Insola, A. and Marotta, R., "Advanced oxidation processes (AOP) for water purification and recovery", ***Catalysis Today***, Vol. 53, No. 1, (1999), 51-59.
4. Nischk, M., Mazierski, P., Gazda, M. and Zaleska, A., "Ordered TiO_2 nanotubes: The effect of preparation parameters on the photocatalytic activity in air purification process", ***Applied Catalysis B: Environmental***, Vol. 144, (2014), 674-685.
5. Wang, G., Chen, S., Yu, H. and Quan, X., "Integration of membrane filtration and photoelectrocatalysis using a TiO_2 /carbon/ Al_2O_3 membrane for enhanced water treatment", ***Journal of Hazardous Materials***, Vol. 299, (2015), 27-34.
6. Xie, T., Sullivan, N., Steffens, K., Wen, B., Liu, G., Debnath, R., Davydov, A., Gomez, R. and Motayed, A., "Uv-assisted room-temperature chemiresistive NO_2 sensor based on TiO_2 thin film", ***Journal of Alloys and Compounds***, Vol. 653, (2015), 255-259.
7. Gonullu, Y., Haidry, A.A. and Saruhan, B., "Nanotubular cr-doped TiO_2 for use as high-temperature NO_2 gas sensor", ***Sensors and Actuators B: Chemical***, Vol. 217, (2015), 78-87.
8. Gong, J., Li, Y., Hu, Z., Zhou, Z. and Deng, Y., "Ultrasensitive NH_3 gas sensor from polyaniline nanograin enchased TiO_2 fibers", ***The Journal of Physical Chemistry C***, Vol. 114, No. 21, (2010), 9970-9974.
9. Yue, W., Pan, Y., Xie, Z., Yang, X., Hu, L., Hong, L., Tong, Y. and Cheng, Q., "Different depositing amount of cuins 2 on TiO_2 nanoarrays for polymer/cuins 2– TiO_2 solar cells", ***Materials Science in Semiconductor Processing***, Vol. 40, (2015), 257-261.
10. Shogh, S., Mohammadpour, R. and Taghavinia, N., "Improved photovoltaic performance of nanostructured solar cells by neodymium-doped TiO_2 photoelectrode", ***Materials Letters***, Vol. 159, (2015), 273-275.
11. Yan, Z., Yu, X., Zhang, Y., Jia, H., Sun, Z. and Du, P., "Enhanced visible light-driven hydrogen production from water by a noble-metal-free system containing organic dye-sensitized titanium dioxide loaded with nickel hydroxide as the cocatalyst", ***Applied Catalysis B: Environmental***, Vol. 160, (2014), 173-178.
12. Caballero, L., Whitehead, K., Allen, N. and Verran, J., "Inactivation of escherichia coli on immobilized TiO_2 using fluorescent light", ***Journal of Photochemistry and Photobiology A: Chemistry***, Vol. 202, No. 2, (2009), 92-98.
13. Banerjee, S., Dionysiou, D.D. and Pillai, S.C., "Self-cleaning applications of TiO_2 by photo-induced hydrophilicity and photocatalysis", ***Applied Catalysis B: Environmental***, Vol. 176, (2015), 396-428.
14. Pinho, L., Rojas, M. and Mosquera, M.J., "Ag– SiO_2– TiO_2 nanocomposite coatings with enhanced photoactivity for self-cleaning application on building materials", ***Applied Catalysis B: Environmental***, Vol. 178, No., (2015), 144-154.
15. Anandan, S., Narasinga Rao, T., Sathish, M., Rangappa, D., Honma, I. and Miyauchi, M., "Superhydrophilic graphene-loaded tio2 thin film for self-cleaning applications", ***ACS Applied Materials & Interfaces***, Vol. 5, No. 1, (2012), 207-212.
16. Czech, B., Buda, W., Pasieczna-Patkowska, S. and Oleszczuk, P., "Mwcnt– TiO_2–SiO_2 nanocomposites possessing the photocatalytic activity in uva and uvc", ***Applied Catalysis B: Environmental***, Vol. 162, No., (2015), 564-572.
17. Im, J.S., Yun, S.-M. and Lee, Y.-S., "Investigation of multielemental catalysts based on decreasing the band gap of titania for enhanced visible light photocatalysis", ***Journal of Colloid and Interface Science***, Vol. 336, No. 1, (2009), 183-188.
18. Elahifard, M.R., Rahimnejad, S., Haghighi, S. and Gholami, M.R., "Apatite-coated Ag/AgBr/TiO_2 visible-light photocatalyst for destruction of bacteria", ***Journal of the American Chemical Society***, Vol. 129, No. 31, (2007), 9552-9553.
19. Hu, C., Lan, Y., Qu, J., Hu, X. and Wang, A., " Ag/AgBr/TiO_2 visible light photocatalyst for destruction of azodyes and bacteria", ***The Journal of Physical Chemistry B***, Vol. 110, No. 9, (2006), 4066-4072.
20. Liu, Q., Ding, J., Mante, F.K., Wunder, S.L. and Baran, G.R., "The role of surface functional groups in calcium phosphate nucleation on titanium foil: A self-assembled monolayer technique", ***Biomaterials***, Vol. 23, No. 15, (2002), 3103-3111.
21. Linsebigler, A.L., Lu, G. and Yates, J.T., "Photocatalysis on TiO_2 surfaces: Principles, mechanisms, and selected results", ***Chemical Reviews***, Vol. 95, No. 3, (1995), 735-758.
22. Ullah, K., Meng, Z.-D., Ye, S., Zhu, L. and Oh, W.-C., "Synthesis and characterization of novel PbS–graphene/ TiO_2 composite with enhanced photocatalytic activity", ***Journal of Industrial and Engineering Chemistry***, Vol. 20, No. 3, (2014), 1035-1042.
23. Yao, Y., Li, G., Ciston, S., Lueptow, R.M. and Gray, K.A., "Photoreactive TiO_2/carbon nanotube composites: Synthesis and reactivity", ***Environmental Science & Technology***, Vol. 42, No. 13, (2008), 4952-4957.
24. Li, G.-S., Zhang, D.-Q. and Yu, J.C., "Visible-light photocatalyst: Cds quantum dots embedded mesoporous TiO_2", ***Environmental Science & Technology***, Vol. 43, No. 18, (2009), 7079-7085.
25. Sajjad, A.K.L., Shamaila, S., Tian, B., Chen, F. and Zhang, J., "Comparative studies of operational parameters of degradation of azo dyes in visible light by highly efficient WOx/TiO_2 photocatalyst", ***Journal of Hazardous Materials***, Vol. 177, No. 1, (2010), 781-791.
26. Lv, K., Li, J., Qing, X., Li, W. and Chen, Q., "Synthesis and photo-degradation application of WO_3/TiO_2 hollow spheres", ***Journal of Hazardous Materials***, Vol. 189, No. 1, (2011), 329-335.
27. Ullah, K., Ye, S., Jo, S.-B., Zhu, L., Cho, K.-Y. and Oh, W.-C., "Optical and photocatalytic properties of novel heterogeneous $PtSe_2$–graphene/TiO_2 nanocomposites synthesized via ultrasonic

assisted techniques", ***Ultrasonics Sonochemistry***, Vol. 21, No. 5, (2014), 1849-1857.

28. Zhang, L., Yu, J.C., Yip, H.Y., Li, Q., Kwong, K.W., Xu, A.-W. and Wong, P.K., "Ambient light reduction strategy to synthesize silver nanoparticles and silver-coated TiO_2 with enhanced photocatalytic and bactericidal activities", ***Langmuir***, Vol. 19, No. 24, (2003), 10372-10380.
29. Vamathevan, V., Amal, R., Beydoun, D., Low, G. and McEvoy, S., "Photocatalytic oxidation of organics in water using pure and silver-modified titanium dioxide particles", ***Journal of Photochemistry and Photobiology A: Chemistry***, Vol. 148, No. 1, (2002), 233-245.
30. Liu, S. and Chen, Y., "Enhanced photocatalytic activity of tio 2 powders doped by Fe unevenly", ***Catalysis Communications***, Vol. 10, No. 6, (2009), 894-899.
31. Nitoi, I., Oancea, P., Raileanu, M., Crisan, M., Constantin, L. and Cristea, I., "Uv–vis photocatalytic degradation of nitrobenzene from water using heavy metal doped titania", ***Journal of Industrial and Engineering Chemistry***, Vol. 21, No., (2015), 677-682.
32. Choi, W., Termin, A. and Hoffmann, M.R., "The role of metal ion dopants in quantum-sized TiO_2: Correlation between photoreactivity and charge carrier recombination dynamics", ***Journal of Physical Chemistry***, Vol. 98, No. 51, (1994), 13669-13679.
33. Asahi, R., Morikawa, T., Ohwaki, T., Aoki, K. and Taga, Y., "Visible-light photocatalysis in nitrogen-doped titanium oxides", ***science***, Vol. 293, No. 5528, (2001), 269-271.
34. Lin, X., Fu, D., Hao, L. and Ding, Z., "Synthesis and enhanced visible-light responsive of c, n, s-tridoped TiO_2 hollow spheres", ***Journal of Environmental Sciences***, Vol. 25, No. 10, (2013), 2150-2156.
35. Herrmann, J.-M., "Heterogeneous photocatalysis: Fundamentals and applications to the removal of various types of aqueous pollutants", ***Catalysis Today***, Vol. 53, No. 1, (1999), 115-129.
36. Cong, Y., Li, X., Qin, Y., Dong, Z., Yuan, G., Cui, Z. and Lai, X., "Carbon-doped TiO_2 coating on multiwalled carbon nanotubes with higher visible light photocatalytic activity", ***Applied Catalysis B: Environmental***, Vol. 107, No. 1, (2011), 128-134.
37. Shaari, N., Tan, S. and Mohamed, A., " Synthesis and characterization of cnt/ce- TiO_2 nanocomposite for phenol degradation", ***Journal of Rare Earths***, Vol. 30, No. 7, (2012), 651-658.
38. Wang, W., Serp, P., Kalck, P. and Faria, J.L., "Visible light photodegradation of phenol on mwnt- TiO_2 composite catalysts prepared by a modified sol–gel method", ***Journal of Molecular Catalysis A: Chemical***, Vol. 235, No. 1, (2005), 194-199.
39. Silva, C.G. and Faria, J.L., "Photocatalytic oxidation of benzene derivatives in aqueous suspensions: Synergic effect induced by the introduction of carbon nanotubes in a TiO_2 matrix", ***Applied Catalysis B: Environmental***, Vol. 101, No. 1, (2010), 81-89.
40. Yen, C.-Y., Lin, Y.-F., Hung, C.-H., Tseng, Y.-H., Ma, C.-C.M., Chang, M.-C. and Shao, H., "The effects of synthesis procedures on the morphology and photocatalytic activity of multi-walled carbon nanotubes/ TiO_2nanocomposites", ***Nanotechnology***, Vol. 19, No. 4, (2008), 045604.
41. Song, Z., Hrbek, J. and Osgood, R., "Formation of TiO_2 nanoparticles by reactive-layer-assisted deposition and characterization by xps and stm", ***Nano Letters***, Vol. 5, No. 7, (2005), 1327-1332.
42. Akhavan, O., Abdolahad, M., Abdi, Y. and Mohajerzadeh, S., "Synthesis of titania/carbon nanotube heterojunction arrays for photoinactivation of E. Coli in visible light irradiation", ***Carbon***, Vol. 47, No. 14, (2009), 3280-3287.
43. Yang, K., Dai, Y., Huang, B. and Whangbo, M.-H., "Density functional characterization of the visible-light absorption in substitutional C-Anion- and C-Cation-Doped TiO_2", ***The Journal of Physical Chemistry C***, Vol. 113, No. 6, (2009), 2624-2629.
44. Lim, M., Zhou, Y., Wood, B., Guo, Y., Wang, L., Rudolph, V. and Lu, G., "Fluorine and carbon codoped macroporous titania microspheres: Highly effective photocatalyst for the destruction of airborne styrene under visible light", ***The Journal of Physical Chemistry C***, Vol. 112, No. 49, (2008), 19655-19661.
45. Woan, K., Pyrgiotakis, G. and Sigmund, W., "Photocatalytic carbon-nanotube– TiO_2 composites", ***Advanced Materials***, Vol. 21, No. 21, (2009), 2233-2239.
46. Chen, Y., Crittenden, J.C., Hackney, S., Sutter, L. and Hand, D.W., "Preparation of a novel TiO_2-based p– n junction nanotube photocatalyst", ***Environmental Science & Technology***, Vol. 39, No. 5, (2005), 1201-1208.

Synthesis and Characterization of Anatase-coated Multiwall Carbon Nanotube for Improvement of Photocatalytic Activity

F. Kordhaghi, S. K. Sadrnezhaad

Department of Materials Science and Engineering, Sharif University of Technology, Tehran, Iran

P A P E R I N F O

Paper history:
Received 22 May 2016
Received in revised form 09 February 2017
Accepted 09 February 2017

Keywords:
Nano-photocatalyst
Anatase
Titanium Dioxide
Carbon Nanotube
Nanocomposite

چکیده

پوشش دادن تیتانیای آناتاز گونه به روش سل-ژل هم‌رسوبی بر نانولوله کربنی (CNT) سبب افزایش سطح ویژه و بهبود خواص فتوکاتالیستی تیتانیا شد. رسانایی بالستیک نانولوله‌های کربنی همراه با نیمه‌رسانا بودن آناتاز در دمای اتاق باعث حدود ۳۷٪ بهبود در خواص فتوکاتالیستی نسبت به بالاترین توان رنگ‌بری متیل اورانژ شد. برای مشخصه‌یابی و تعیین بازدهی فتوکاتالیستی، از پراش اشعه ایکس(XRD) ، میکروسکوپ الکترونی روبشی نشر میدانی(FESEM) ، طیف-سنجی فوتوالکترون اشعه ایکس (XPS)، طیف‌سنجی انتشار بازتاب (DRS) و طیف‌سنجی با اشعه ماوراء بنفش-مرئی (UV-Vis)استفاده شد. اتصال نانوذرات آناتاز بر نانولوله‌های عامل‌دار شده به مقدار ۳۰٪ سبب رنگ بری ۹۹/۷۲ درصدی متیل اورانژ در اثر ۱۶۰ دقیقه تابش با لامپ ماوراء بنفش ۸ وات شد. این مقدار چهار برابر بیشتر از نانوذرات TiO_2 خالص و بسیار بیشتر از مقادیر گزارش شده در مقالات قبلی بود. علت این بهبود، سطح ویژه بزرگ‌تر، بازترکیب کمتر بار، ساختار بلوری اصلاح شده و جابه‌جا شدن طیف‌های جذبی به سمت نور مرئی به واسطه ایجاد پیوند Ti−O−C تشخیص داده شد.

***doi**: 10.5829/idosi.ije.2017.30.04a.12*